Toxicology in Vitro 69 (2020) 104996

Contents lists available at ScienceDirect

Toxicology in Vitro

journal homepage: www.elsevier.com/locate/toxinvit

Development of a 96-well based assay for kinetic determination of catalase enzymatic-activity in biological samples

Luís F. Grilo[a], João D. Martins[a], Chiara H. Cavallaro[a], Peter W. Nathanielsz[b], Paulo J. Oliveira[a], Susana P. Pereira[a,c,*]

[a] CNC- Center for Neuroscience and Cell Biology, UC-Biotech Building, Biocant Park, Cantanhede, Portugal
[b] Department of Animal Science, College of Agriculture and Natural Resources, Laramie, WY, USA
[c] Research Centre in Physical Activity, Health and Leisure (CIAFEL), Faculty of Sport, University of Porto, Porto, Portugal

ARTICLE INFO

Keywords:
Catalase
Toxicity screening
Hydrogen peroxide
Oxidative stress
Antioxidant defense

ABSTRACT

Oxidative stress biomarkers are powerful endpoints in toxicological research. Cellular reductive/oxidative balance affects numerous signaling pathways involving H_2O_2. Detoxification and control of H_2O_2 levels results mainly from catalase activity.

The aim of this work was to develop a precise, simple, cost-effective microassay to measure catalase activity in small tissue samples and cell extracts.

We developed a protocol that quantifies H_2O_2 decomposition by intrinsic catalase in biological samples. Catalase activity was calculated based on rate of decomposition of H_2O_2, following absorbance at 240 nm. We developed a multi-well spectroscopic approach, reducing sample quantity requirements and allowing simultaneous assessment of large number of samples.

The protocol is sensitive across a wide range of catalase activity (11.5–7575 U). The assay presents a 95% confidence interval with an intra-assay coefficient of variation of 3.7%, an inter-assay coefficient of variation of 6.2% and good correlation with a commercial kit. The assay was established and validated for different biological samples, including sheep hepatic tissue and human tumor and non-tumor cell lines.

This high-throughput method is robust, sensitive, time-saving and cost-effective, generating highly reproducible results with precision and good correlation with a commercial kit reinforcing the method's validity for research and toxicological applications.

1. Introduction

Oxidative stress is a major mechanism involved in several pathologies and in the toxicity of different xenobiotics (Lennicke et al., 2015; Machado et al., 2010; Sepasi Tehrani and Moosavi-Movahedi, 2018). Cellular reductive/oxidative balance affects numerous signaling cascades which involve hydrogen peroxide (H_2O_2). H_2O_2 plays different signaling roles but is also associated with potential deleterious toxicological and pathological effects (Sepasi Tehrani and Moosavi-Movahedi, 2018). Detoxification and control of H_2O_2 levels results mainly from catalase activity. A number of drugs and other xenobiotics affect catalase activity (Glorieux et al., 2015).

Catalase is ubiquitously present in aerobic organisms. Catalases are divided in three main groups based on their structure and function: true catalases; catalase-peroxidases; and manganese catalases (Glorieux and Calderon, 2017). Although their distribution is ubiquitous, catalase activity is usually higher in liver, kidneys and red blood cells. While catalase is generally present in peroxisomes, its constitutive presence in rat liver and heart mitochondria is reported, contributing to detoxification of H_2O_2 (Radi et al., 1991; Salvi et al., 2007). H_2O_2 is typically produced by specialised cells such as neutrophils, as a defense against pathogens, and as a by-product of reactions catalyzed by enzymes such as mitochondrial monoamine oxidases (Marinho et al., 2014). However, a major source of H_2O_2 is detoxification of superoxide anion ($^{\bullet}O_2^-$) by mitochondrial superoxide dismutase (SOD2) or by cytosolic SOD1 (Dunning et al., 2013). The cytochrome P450-dependent electron transport systems and mitochondrial electron transport chain (ETC) are important endogenous sources of reactive oxygen species (ROS), being

Abbreviations: ATP, adenosine triphosphate; ETC, electron transport chain; ROS, reactive oxygen species; SOD, superoxide dismutase; CN, sodium cyanide; 2ME, 2-mercaptoethanol; 3AT, 3-amino-1,2,4-triazole; SA, sodium azide; CatBL, purified catalase from bovine liver

* Corresponding author at: CNC-Center for Neuroscience and Cell Biology, UC Biotech, Biocant Park, University of Coimbra, 3060-197 Cantanhede, Portugal.
E-mail addresses: peter.nathanielsz@uwyo.edu (P.W. Nathanielsz), pauloliv@ci.uc.pt (P.J. Oliveira), pereirasusan@gmail.com (S.P. Pereira).

https://doi.org/10.1016/j.tiv.2020.104996
Received 14 May 2020; Received in revised form 31 August 2020; Accepted 3 September 2020
Available online 06 September 2020
0887-2333/

Table 1
List of experimental catalase assays available.

Method	Description	Reference
Ultraviolet spectroscopy	H_2O_2 decomposition by catalase is followed by ultraviolet spectroscopy. **Limitations:** requires high amount of sample and only allows to measure one sample without replicates each time.	Aebi (Aebi, 1984)
Titrimetric method	Proposed for tissues with low levels of catalase. Low sources of error were described. **Limitations:** presented low reliability due to the high amount of sample required and presented low precision.	Aebi (Aebi, 1984)
Manometric method	Catalase-activity is measured by following O_2 production. Easy, rapid and inexpensive assay. **Limitations:** this is not ideal to follow kinetics with considerable rigor. Only one sample without replicates can be measure each time.	Teixeira and Mota (Teixeira and Mota, 1992)
Gel-based method	Catalase-activity is followed by gel decomposition. Requires far less sample quantities compared to previous methods. **Limitations:** this is a gel-based method that only provides a qualitative rather than a quantitative result.	Weydert and Cullen (Weydert and Cullen, 2010)
Chemiluminescence method	Catalase-activity is measured through the chemiluminescence signal of H_2O_2-sensitive CdTe quantum dots. Allows sensitive and quick determination of catalase-activity. **Limitations:** this requires a luminescence reader and an intermediate reaction between H_2O_2 and CdTe quantum dots. The assay is more expensive due to the use of CdTe quantum dots.	Ghavamipour 2018 (Ghavamipour et al., 2018)

the ETC considered the major source of $^{\bullet}O_2^-$, under pathological conditions, indirectly contributing to cellular generation of H_2O_2 (Paradies et al., 2014; Bhatti et al., 2017).

H_2O_2 also acts as a transcription-independent signaling molecule, governing redox sensing and regulation, whose importance is comparable to Ca^{2+} or ATP (Sies, 2017). In multicellular organisms several transcription factors are regulated by H_2O_2 (Marinho et al., 2014). It is thought that catalase plays a major role in maintaining physiological concentrations of H_2O_2, avoiding its cytotoxic effects and externalization as a threat signal (Nenoi et al., 2001; Veal et al., 2007; Schieber and Chandel, 2014; Moloney and Cotter, 2018).

Measurement of catalase activity is an important and useful parameter to better understand the redox status of biological samples and assess the toxicity of different xenobiotics. Table 1 shows the most common currently used methods to measure catalase activity and some of their inherent limitations (Aebi, 1984; Teixeira and Mota, 1992; Weydert and Cullen, 2010).

In the present work, we developed a 96-well plate-based microassay to measure catalase activity from small amounts of tissue and cells in a highly specific, rapid and precise way. We optimized the assay for homogenized sheep liver tissue and HepG2 cell lysates, which were previously associated with high levels of catalase protein expression and activity (Zhao et al., 2019; Ibrahim et al., 2000), taking into account the H_2O_2 ultraviolet spectroscopic characteristics and the adptation to a multiplate format to improve assay's performance. The goal was to develop a reliable and reproducible 96-well plate-based microassay for kinetic determination of catalase enzymatic activity, easy to adapt to other sample types, with low intra- and inter-variation.

2. Materials and methods

2.1. Materials

The list and preparation of reagent solutions is presented in supplementary material.

2.2. Sample preparation

Cell and tissue sample preparation is presented in supplementary material.

2.3. Catalase enzymatic assay

The assay consists in the reaction of 20 μL of sample with 100 μL of H_2O_2 solution in a 300 μL final reaction volume. Each well was prepared according to Table 2 and Fig. S1. Catalase activity was measured by adding H_2O_2 to the samples and following its decomposition over time by 240 nm absorbance (Aebi, 1984). To ensure that the method is working properly and is specific for catalase dependent H_2O_2 degradation, several controls were performed (Table 2).

A 240 nm initial basal absorbance was determined for background correction and protein loading assessment. Subsequently, 100 μL of phosphate buffer 50 mM, pH = 7.8 (PB) was added to columns 1 and 12 (Table 2 last line). Next, using a multichannel, 100 μL of H_2O_2 solution 90 mM was added simultaneously to columns 2–11 immediately before starting the kinetic reading. Catalase activity was followed by the variation of H_2O_2 absorbance at 240 nm during 2.5 min, with a readout each 15 s using a Cytation3 multi-mode microplate reader (BioTek Instruments, Inc.,Winooski,VT,USA). A typical catalase reaction/H_2O_2 degradation is shown in Fig. 1A.

2.4. Catalase inhibitors

Sodium azide (SA), 2-mercaptoethanol (2ME) and 3-amino-1,2,4-triazole (3AT) were tested as catalase-activity inhibitors. Several inhibitor dilutions were prepared in PB and incubated with 20 μL of 100 μg/mL sheep liver samples or with 75 mg of commercial purified catalase from bovine liver (CatBL). Samples from 5 independent homogenized sheep livers were assayed in triplicates. Final concentrations of 0.1, 0.5, 1, 5, 10 and 25 mM were tested for 3AT (with and without 2 h ice-incubation) and 2ME, and 0.1, 0.25, 0.5, 0.75, 1 and 10 mM for SA.

2.5. Data analysis

Maximal catalase activity was obtained by performing an exponential regression on the first seven kinetics points, from 0-90s. The first 15 s of the exponential regression were used to perform a linear regression whose slope represents catalase maximal-activity in Units (detailed description in supplementary material).

2.6. Statistics

Statistical analysis were performed using GraphPad Prism6 (San Diego, CA, USA) with group comparisons using the paired or unpaired *t*-test for samples from the same or independent sources, respectively. Comparisons with $p \leq 0.05$ were considered statistically different.

3. Results

The typical catalase kinetics obtained with this method are shown in Fig. 1A. Catalase saturation occurs after 2.5 min following which the reaction rate remains constant which do not represent catalase maximal activity. The positive and negative controls (Fig. 1B) increased the protocol's robustness and reliability.

Table 2
Solutions required for loading the plate during the assay and respective experimental quality controls.

	Assay	Positive Control		Negative Controls					
		Pure Catalase	BSA	Without H_2O_2			With Catalase inhibitor		
				BSA	Pure catalase	Sample	BSA	Pure catalase	Sample
	A	B	C	D	E	F	G	H	I
Sample solution	20 µL	–	–	–	–	20 µL	–	–	20 µL
Fresh catalase solution (37.5 µg/mL)	–	20 µL	–	–	20 µL	–	–	20 µL	–
BSA solution (200 µg/mL)	–	–	20 µL	20 µL	–	–	20 µL	–	–
Phosphate buffer (50 mM, pH 7.8)	180 µL	180 µL	180 µL	180 µL	180 µL	180 µL	–	–	–
Sodium azide solution (1.25 mM)	–	–	–	–	–	–	180 µL	180 µL	180 µL
H_2O_2 solution (90 mM)	100 µL	100 µL	100 µL	–	–	–	100 µL	100 µL	100 µL
Phosphate buffer (50 mM, pH 7.8)	–	–	–	100 µL	100 µL	100 µL	–	–	–

Experimental quality controls		**Objective**
B	**Catalase solution with H_2O_2**	A positive control to ensure that the experimental strategy is working
C	**BSA solution with H_2O_2**	Observe eventual decreases in absorbance caused by interactions between H_2O_2 and proteins.
D	**BSA solution without H_2O_2**	Same as control E with a protein unrelated to the measured endpoint.
E	**Catalase solution without H_2O_2**	See if there are differences of the absorbance caused by changes in catalase. It represents the basal level to control B.
F	**Sample without H_2O_2**	Determine differences between samples' absorbance and ensure their stability throughout the assay
G	**BSA solution with sodium azide and H_2O_2**	Measure the basal absorbance of all the wells with H_2O_2 and catalase inhibitor
H	**Catalase solution with sodium azide and H_2O_2**	A negative control to access catalase inhibition.
I	**Sample with sodium azide and H_2O_2**	Assess catalase inhibition in the samples and the contribution of other enzymes to the detoxification of H_2O_2.

The protein amount of sheep liver homogenate was also optimized (Fig. 1C). The confidence range, at which the ratio between catalase activity and sample amount remains constant, was between 125 ng-2 µg of protein. A confidence range between 16 and 100 µg was determined for HepG2 cells lysates (Fig. 1D). Since catalase activity and expression vary between different cell lines or tissues (Ibrahim et al., 2000), sample's-specific confidence range for catalase activity determination should be performed. Additionally, a very high catalase activity may lead to excessive oxygen release during the assay resulting in bubble formation compromising absorbance measurements.

Several protocols were tested to enhance hepatic sample extraction yield for the catalase assay. Two homogenization apparatuses were compared, Ultra-TurraxT10 and Potter-Elvehjem (Fig. 1E). The Ultra-TurraxT10 proved to be more advantageous, allowing to work with smaller amount of tissue sample in a faster manner. While ultra-sonication increased the extraction yield, the use of 1% Triton®X-100 detergent in the extraction buffer did not increase the yield of the extraction (Fig. 1F) and can interfere with the assay since it absorbs at 240 nm.

Positive and negative controls were performed to increase the robustness of the protocol. As a negative control catalase inhibitors were used, namely sodium cyanide (CN), 2-mercaptoethanol (2ME), 3-amino-1,2,4-triazole (3AT) and sodium azide (SA)(Fig. 2, Table S1) (Glorieux and Calderon, 2017; Jakopitsch et al., 2003; Terada, M. [Sodium azide], 2004; Switala and Loewen, 2002; Dawson, 1990; Takeda et al., 1980). As an initial technical control, the absorption spectra of inhibitors' solutions were obtained to determine interferences at 240 nm absorbance. All tested inhibitors showed absorbance at 240 nm.

Although 2ME resulted in total catalase inhibition, it was not catalase-specific so it was considered not suitable. SA and 3AT showed high catalase inhibition (Fig. 2B,D). 3AT requires a 2 h-incubation with catalase to be effective, therefore its utilization would increase the time of the assay which could compromise catalase activity. Although SA is not as specific as 3AT, based on literature, we did not find any other enzyme prone to inhibition by SA interaction and able to react with H_2O_2 (Dunning et al., 2013).

CatBL was included in the assay as a positive control. Protein amount was optimized accounting for two parameters (**Fig.** S2): the initial kinetic catalase-activity assay 240 nm-absorbance must not be lower than 1; and triplicates for the same protein amount should be highly consistent. The first parameter ensures that low H_2O_2 was consumed in the interval between plate pipetting and the start of the reading. The second parameter allows for the minimization of pipetting errors arising from the utilization of under- or over-diluted catalase solutions. We observe a large inconsistency for catalase determination using 0.5 µg CatBL. Above this concentration there is less variation in the determination of catalase-activity for identical preparations, with the highest activity observed for 0.8 µg (Fig. S2A).

The stability of CatBL to undergo freezing and thawing once dissolved in PB was also addressed. We observed that catalase activity is diminished by this procedure ($p = 0.008$; Fig. S2B). Therefore, freshly prepared pure catalase solutions should be used as positive controls.

In contrast to CatBL activity, catalase activity in sheep liver extracts remained unchanged after 10 freeze/thaw cycles (Fig. 2E), provided samples were always kept on ice during extraction and handling and immediately frozen at −20 °C. Unlike the observed maintenance of catalase activity in sheep liver extracts, catalase activity from HepG2 extracts decreased after frozen and thawed (Fig. 2F).

To test the assay sensibility of *in vitro* catalase activity modulation (Fig. 2G), HepG2 cells were treated with oxidative stress inducers H_2O_2 (1 mM, 3 h), t-BHP (500 µM, 3 h) and menadione (5 µM, 3 h) (Lim et al., 2018; Al-Suhaimi, 2014), catalase inhibitor 3-AT (10 mM, 24 h) (Zhao et al., 2019) and rotenone (25 µM, 3 h) (Siddiqui et al., 2013). The catalase inhibitor 3-AT caused a 72% inhibition of catalase activity, while 25 µM rotenone lead to a 20% catalase activity inhibition. A similar catalase activity stimulation occurred with 500 µM t-BHP and 5 µM menadione (22%) while we observed a 27% increased catalase activity with 1 mM of H_2O_2.

We also improved data analysis for a trustful catalase maximal activity measurement. We demonstrated that the best approach is approximating the results firstly to the exponential curve instead of obtaining the slope directly from a linear regression to the experimental readings. This alteration allows to get higher activities closer to the real maximal activity of the sample, best approximations (higher R^2 in the regression) and increases the range of protein amount that can be reliable used in the assay (Fig. 3A,B).

The assay performance was evaluated based on its sensitivity and precision as determined using CatBL. The slopes obtained by the method are inversely proportional to catalase activity, meaning that a more

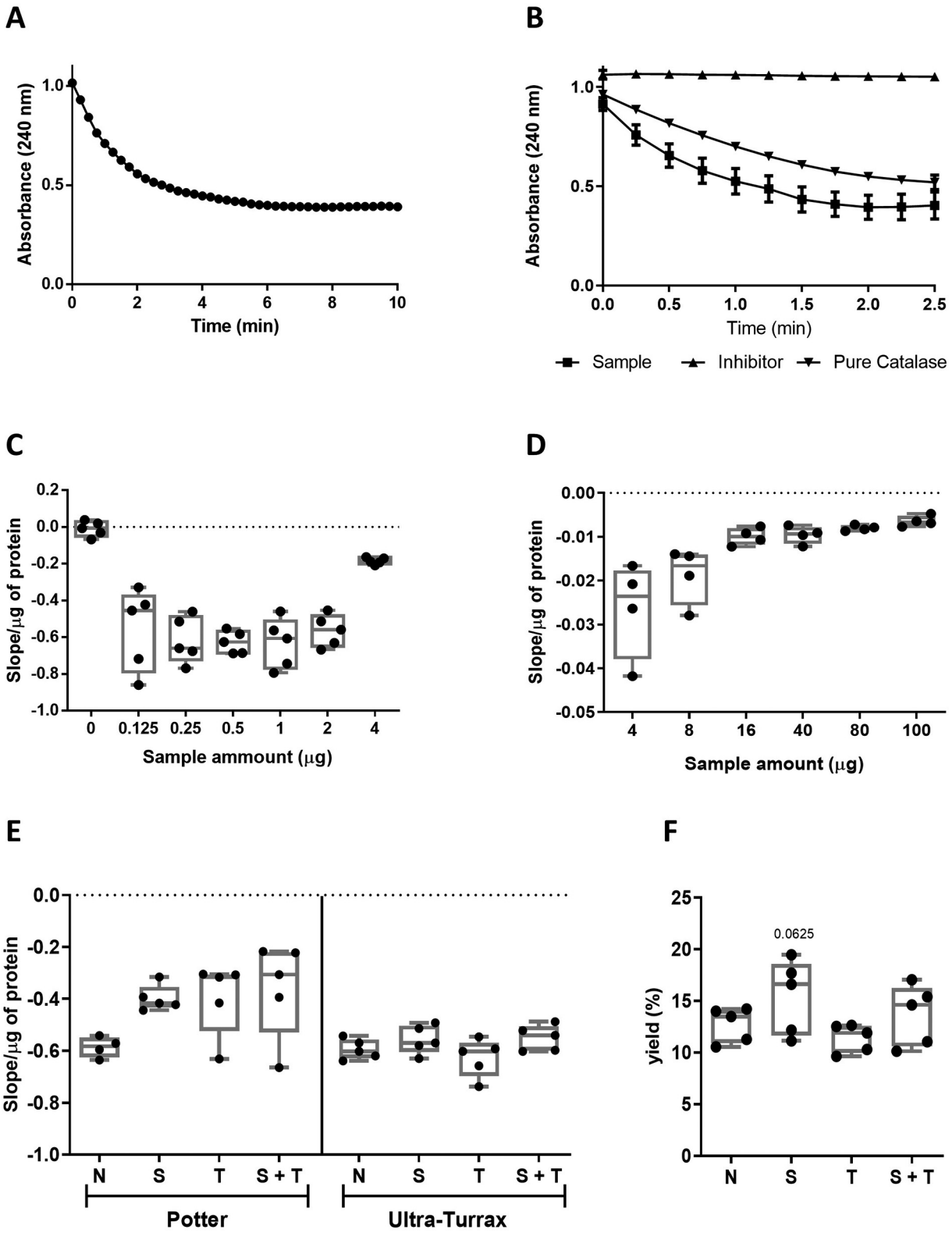

Fig. 1. Results from catalase activity assays and protocol optimization: A) alteration of absorbance at 240 nm after H_2O_2 addition to catalase-containing samples during 10 min and B) typical result of an assay of a catalase-containing sample and a positive (pure catalase) and negative control (inhibitor). Optimization of the protein confidence range to perform the catalase kinetic assay in C) sheep liver homogenates and D) HepG2 lysates samples. The assay was performed in triplicate on 5 independent samples of sheep liver homogenates and 4 independent collections of HepG2 cells lysates. The effect of protein extraction method in sheep liver homogenates in E) maximal catalase activity and F) the percentage of extraction yield, defined as the protein obtained as percentage of the initial weight of the tissue. Experiments were performed in 5 independent sheep liver homogenates. N – Mechanical homogenization; S- addition of a ultrasonication step; T – Addition of 1% Triton®X-100 to the extraction buffer; S + T – Addition of a ultrasonication step and 1% Triton®X-100 to the extraction buffer.

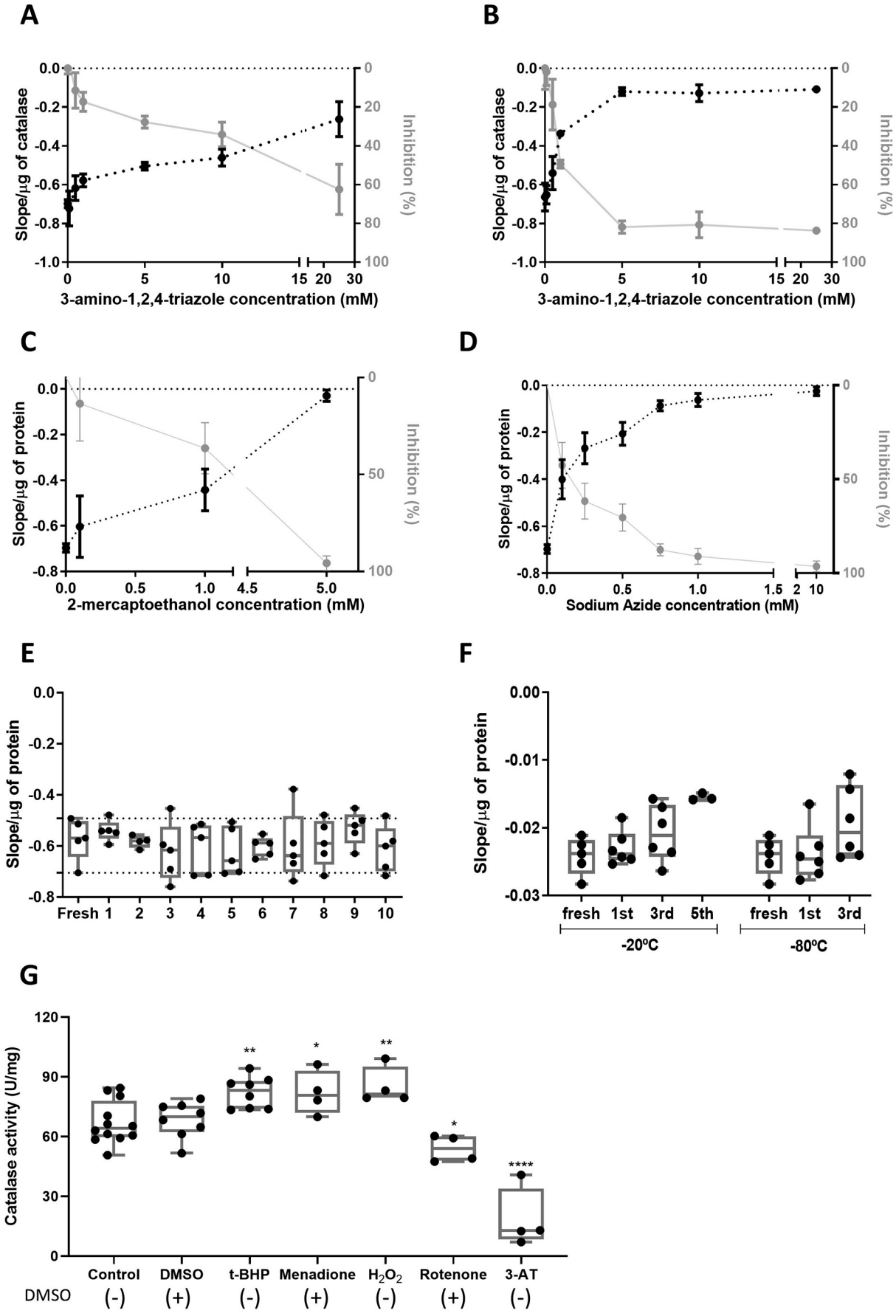

(caption on next page)

Fig. 2. Optimization of negative (inhibitor) control, effect of freezing samples and *in vitro* catalase activity modulation. Variation of catalase activity with different concentrations of inhibitors: A) 3-amino-1,2,4-triazole without incubation period, B) 3-amino-1,2,4-triazole with 2 h incubation period at 4°C, C) 2-mercaptoethanol and D) sodium azide. The assays were performed with CatBL and 3 independent samples of sheep liver homogenates (presented) with concordant results. Catalase activity of E) liver sheep extractions and F) HepG2 cell lysates after freezing cycles. Five samples from the same extraction of sheep liver homogenates and six HepG2 samples were used in the assays and aliquots. *In vitro* modulation of catalase activity G) by oxidative stress inducers and catalase inhibitors in HepG2 cell lysates ($n = 4$; unpaired *t*-test: * $p < 0.05$, ** $p < 0.01$, **** $p < 0.0001$). All experiments were run in triplicate for catalase activity.

negative slope value represents higher catalase activity, and decrease linearly between 2 ng and 2 μg of CatBL, which corresponds to 11.5 and 7575 catalase units (Fig. 3C). However, after normalization for protein, linearity was only observed for more than 50 ng of catalase (Fig. 3D). For samples with low catalase activity, we suggest running the kinetic assay for 20 min and using the linear part of the kinetic curves to calculate the slope and catalase maximal activity. Special care must be taken to adapt the controls performed in the assay to a 20 min kinetic assay namely, to adjust the quantity of CatBL used as positive control.

The precision of the method was determined by performing 45 repetitions of assays using the same CatBL preparation. A mean 95% confidence interval with 3.75% intra-assay coefficient of variation was obtained. Precision between assays was determined by quantifying CatBL solutions activity on three different days, running triplicates each day. The observed variation in catalase-activity inter-assays was 6.25%.

In addition, we performed the protocol proposed here comparing it with a commercial kit (Cayman cat.:707002, Ann Arbor,MI,USA) on 15 independent samples of sheep liver homogenates from same extraction. We observed a good correlation between samples measured through Pearson correlation ($r = 0.73$) (Fig. 3E). Catalase activity presented a weak correlation with the catalase protein expression ($r = 0.21$) in 15 independent sheep liver homogenates, probably due to the post-translational alterations that catalase can suffer (Fig. 3F) (Cao et al., 2003a). The protocol was also tested and validated for other human cell lines: Skin Fibroblasts, BT20 and MCF-7AZ.

4. Discussion

The catalase ability to deal with high concentrations of H_2O_2 is a good marker of cell' health that can be used to determine xenobiotics toxicity. Alterations in catalase activity have been reported in multiple human diseases (Glorieux et al., 2015; Glorieux and Calderon, 2017). In mice, cardiac catalase activity and expression are rapidly increased to prevent the oxidative damage when animals are fed with a high-fat diet (Glorieux and Calderon, 2017; Rindler et al., 2013; Halliwell and Gutteridge, 2015). Xenobiotics and drugs can also modulate catalase activity by directly interfering with the catalytic center, by changing hydrogen peroxide intracellular levels or by activating signaling pathways that induce catalase posttranslational modifications (Cao et al., 2003a; Rafikov et al., 2014; Cao et al., 2003b; Yan and Harding, 1997; Furuta et al., 1974).

Flavonoids and insecticides among other xenobiotics inhibit catalase activity in *in vitro* studies (Krych and Gebicka, 2013; Gargouri et al., 2020; Maćczak et al., 2017). In other hand, molecules as endothelin-1, retinoic acid and pioglitazone stimulate catalase activity (Rafikov et al., 2014; Pasquali et al., 2008; Yekta et al., 2017). Table 3 summarizes described catalase activity variation in the presence of several xenobiotics.

In the presence of high levels of H_2O_2 catalase activity is inhibited (Sepasi Tehrani and Moosavi-Movahedi, 2018). It was demonstrated at the cellular level that with excessive H_2O_2, catalase is phosphorylated and targeted to degradation, increasing oxidative damage through Fenton reaction and promoting cell death (Cao et al., 2003a). Drugs that interfere with intracellular levels of H_2O_2 also modulate catalase activity (Sepasi Tehrani and Moosavi-Movahedi, 2018; Glorieux and Calderon, 2017).

Our protocol of catalase activity determination can be applied to test different xenobiotics *in vitro* or *in vivo* effects and become an essential tool for analytical toxicological research, providing a sensitive and robust way to better understand xenobiotic-induced toxicity and the role of catalase in a variety of toxicological situations. This assay can also be adapted to analyze the efficiency of nanoparticles consisting in catalase-like enzymes and evaluation of biological catalase supplementation (Li et al., 2017; Mu et al., 2012; Kubota et al., 2004; Zhen et al., 2018).

The proposed protocol is ideal for small and critical samples, providing quantitative, reliable and reproducible results. Furthermore, the assay presents kinetic results that can be quickly acquired running two samples simultaneously in triplicate and with appropriate controls. Thus, it is ideal for use when there are a large number of different samples to read. Furthermore, the assay directly measures H_2O_2 degradation and, therefore, any interference due to the formation of intermediate molecules is ruled out. This is a clear advantage comparing to other assays, including the chemiluminescence method and the majority of the commercial kits available.

The amount of sample needed is very different between sheep liver homogenates and HepG2 cells extracts. The amount of protein can vary among different tissues and cell lines which differ in the levels of catalase activity and/or expression (Table S2).

In this study, we used several positive and negative controls which are indispensable to corroborate the specificity, reliance and precision of the measured maximal catalase activity. Controls F and I (Table 2), which represent the negative controls for each sample, were ran for all the samples to be tested according to our plate layout suggested in Fig. S1. The other controls were made only once daily to ensure that all solutions were well prepared and ready to use, preventing the waste of sample.

SA was the inhibitor that showed total inhibition of catalase activity with lower interference (smaller concentrations) with the wavelength of the assay and not requiring pre-incubation. Therefore, we recommend SA use as catalase inhibitor during the assays. However, other inhibitors can also be used at the concentrations that present total inhibition of catalase activity in Fig. 2A-D. Concentrations above the ones tested are not suitable since they present interference in absorbance at 240 nm, decreasing the sensitivity of the assay.

The described assay presented sensibility to *in vitro* catalase activity modulation (Fig. 2G). We observed a 20% inhibition by 25 μM rotenone and 72% inhibition with 10 mM 3-AT similar results to previous reported (Siddiqui et al., 2013; Zhao et al., 2019). We were also able to increase catalase activity with 500 μM t-BHP as described before (Alía et al., 2005). Increase in catalase activity can be attributed both to post-transactional modifications, including phosphorylation (Cao et al., 2003a), or by increased protein expression which can be attributed to several transcription factors, *e.g.* Sp1, NF-Y, XBP1, C/EBPβ the FOX family members FOXO and FOXM1 and PPARγ. In addition, the importance of coactivators such as PGC-1α and Sirt1 and of humoral factors acting, for example, through progesterone and estrogen receptors has also been acknowledged. The regulation of catalase gene transcription isn't yet fully characterized and many other transcription factors, for example Nrf2, OCT-1 or JunB, might as well participate in this process. However, experimental data to confirm their importance is still lacking or inconclusive (Glorieux et al., 2015; Glorieux and Calderon, 2017; Nenoi et al., 2001). Menadione was described as a Nrf2 activator (Herpers et al., 2016) which might explain the observed increase of catalase activity (Fig. 2G).

All the assays were performed in triplicate to exclude outlier results or other artifacts that may occur, as formation of oxygen bubbles that can appear during the assay affecting the exponential shape predicted for the absorbance *vs* time curve. It is possible to run two samples at the same time in each line to a total of 14 samples/plate. We would propose that investigators run paired samples from different experimental groups to reduce the impact of inter-assay variation.

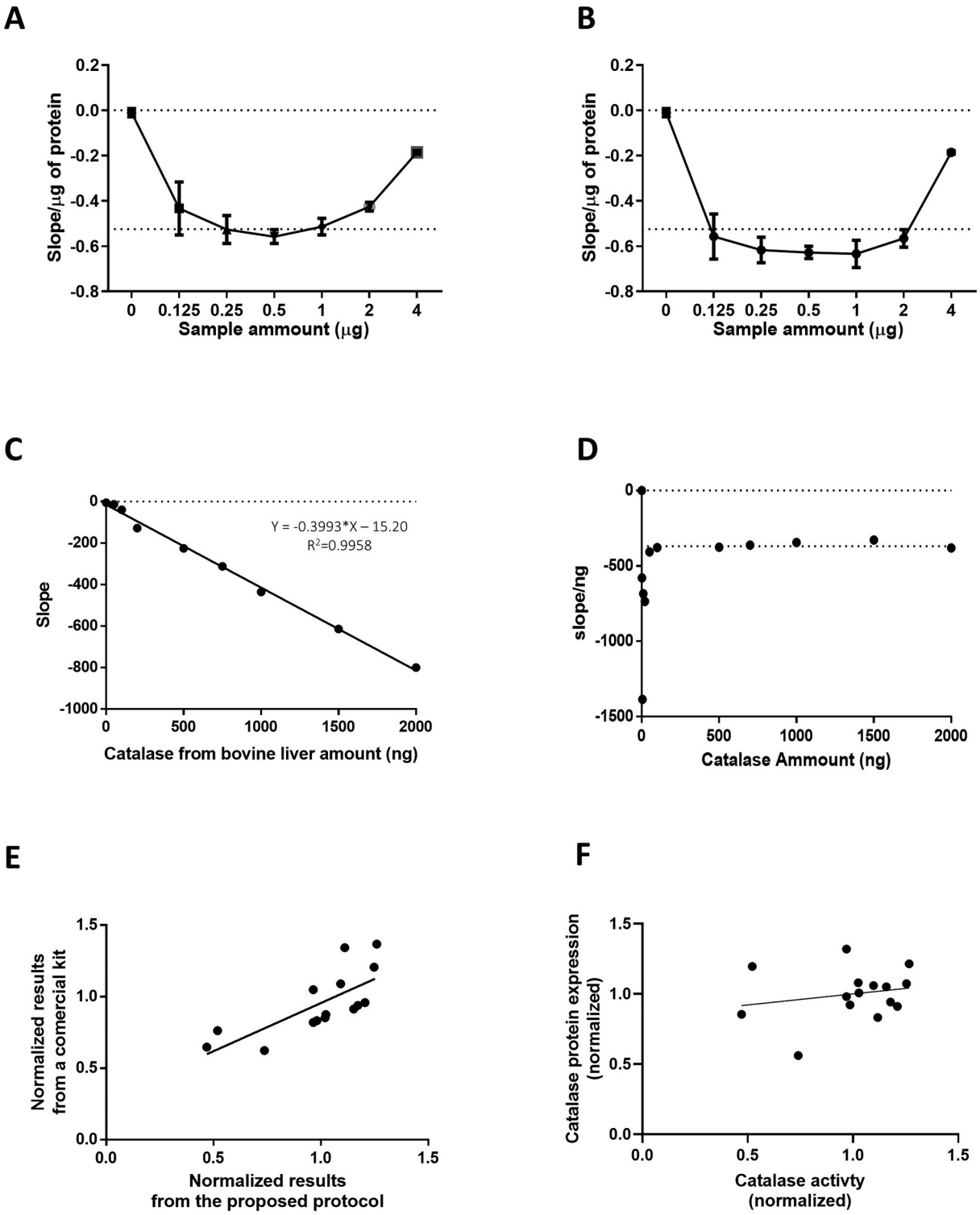

Fig. 3. Effect of the analysis in the obtained data and evaluation of several parameters of the developed protocol. Alternative results depending on the mathematical analysis of the experimental data. Panel A) shows the slopes of 240 nm absorbance decay obtained by linear regression of the experimental readings during the first 60s of the assay. On the right panel B) a non-linear regression was used to fit the experimental data of the initial 90s of assay. Afterwards, the slope for the first 15 s of catalase reaction was obtained using points obtained from the non-linear regression curve. Variation of slope in function of catalase amount. Panel C) shows the linear correlation between catalase amount used and the catalase-activity (slope) measured. The ratio between the measured slope and the CatBL amount used in the respective assay is shown in Panel D). A horizontal linear correlation between this ratio and the catalase amount allows for the defining of a confidence range where the assay results are independent of the catalase amount utilized. Evaluation of the sensitivity of the assay using CatBL C) before and D) after normalization by protein amount. E) correlation between the results of the same samples using the proposed protocol and a commercial kit ($r = 0.73$) and F) correlation between catalase activity and protein expression ($r = 0.21$).

Table 3
Variation of catalase-activity in the presence of several xenobiotics.

Xenobiotic	Catalase-activity Modulation	Model	Ref
(−)-epicatechin gallate	50% decrease at 29 nM (coincubation)	Bovine liver catalase	(Krych and Gebicka, 2013)
(−)-epigallocatechin	50% decrease at 16.6 μM (coincubation)	Bovine liver catalase	(Krych and Gebicka, 2013)
(−)-epigallocatechin gallate	50% decrease at 330 nM (coincubation)	Bovine liver catalase	(Krych and Gebicka, 2013)
(+)-Catechin	50% decrease at 345 μM (coincubation)	Bovine liver catalase	(Krych and Gebicka, 2013)
1-(4-Chlorophenyl)-benzo-2,5-quinone	40% decrease at 1 and 3 μM (24 h)	HaCaT cell line	(Xiao and Goswami, 2015)
3-(dimethylamino)phenol	37.3% increase at 500 ppm (1 h)	Human erythrocytes	(Bukowska et al., 2007)
3-AT	70% decrease at 5, 10 mM (28 h)	HepG2 cell line	(Zhao et al., 2019)
Allylisopropylacetamide	35.2% increase at 7.1 mM (5 days)	H4-ll-*E*-C3 cell line	(De Luca et al., 1970)
Allylisopropylacetylcarbamide	30%, 100%, and 153% increase at 5.43 mM (1, 2, and 3 days, respectively)	RPM1 2402 cells	(De Luca et al., 1970)
Apigenin	50% decrease at 49 μM (co-incubation)	Bovine liver catalase	(Krych and Gebicka, 2013)
Ascorbate	Decrease at 2 mM and 50 μM (24 h)	F36P cells	(Gonçalves et al., 2013)
Astragalin	50% decrease at 45 μM (coincubation)	Bovine liver catalase	(Krych and Gebicka, 2013)
Atanor® (glyphosate formulation)	57.3% increase at LC20 (24 h)	Hep-2 cell line	(Coalova et al., 2014)
Bifenthrin	Decrease at 5, 10 and 20 μM (24 h)	SK-N-SH human neuroblastoma cells	(Gargouri et al., 2020)
Bioallethrin	32% and 64.5% decrease at 100 and 200 μM, respectively (4 h)	Human erythrocytes	(Arif et al., 2020)
Bisphenol A	17%, 24% and 35% decrease at 100, 250 and 500 μg/mL (4 h); and 11%, 11% and 16% decrease at 25, 50 and 100 μg/mL (24 h), respectively	Human erythrocytes	(Maćczak et al., 2017)
Bisphenol AF	14% and 25% decrease at 25 and 100 μg/mL (4 h); and 18% and 13% increase at 0.5 and 5 μg/mL (24 h)	Human erythrocytes	(Maćczak et al., 2017)
Bisphenol F	22% and 33% decrease at 250 and 500 μg/mL (4 h); and 16%, 17% and 22% decrease at 25, 50 and 100 μg/mL (24 h)	Human erythrocytes	(Maćczak et al., 2017)
Bupropion	62% decrease at 150 mg/kg (1 h)	Mice striatum	(Macêdo et al., 2005)
Bupropion	51% decrease at 150 mg/kg (1 h)	Mice prefrontal cortex	(Macêdo et al., 2005)
Catechol	50% decrease at 16 μM (coincubation)	Bovine liver catalase	(Krych and Gebicka, 2013)
Chrysoidine	Decrease (max −50%) at 20 μM (20, 60 and 80 min) and at 50 and 100 μM (20, 40, 60 and 80 min)	Bovine liver catalase	(Yang et al., 2013)
Cisplatin	62.7% decrease at 5 mg/kg daily dose (5 days)	Mouse kidney	(Ghosh et al., 2013)
Cocaine	60% decrease at 10 and 30 mg/kg (1 h)	Mice striatum	(Macêdo et al., 2005)
Dehydroascorbate	Decrease at 2 mM and 50 μM (24 h)	F36P cells	(Gonçalves et al., 2013)
Diclofenac Sodium	50% decrease at 1.8 mM (coincubation)	Human skin	(Altikat et al., 2006)
Doxorubicin	44.5% decrease at 0.2 μM daily dose (5 days)	H9c2 cell line	(Shabalala et al., 2019)
Endothelin-1	180% increase at 100 nM (4 h)	PAEC cell line	(Rafikov et al., 2014)
Galangin	50% decrease at 46 μM (coincubation)	Bovine liver catalase	(Krych and Gebicka, 2013)
Gallic acid	50% decrease at 20 μM (coincubation)	Bovine liver catalase	(Krych and Gebicka, 2013)
Impacto® (spray adjuvant)	38% increase at LC20 (24 h)	Hep-2 cell line	(Coalova et al., 2014)
Kaempferol	50% decrease at 1.80 μM (coincubation)	Bovine liver catalase	(Krych and Gebicka, 2013)
Ketoprofen	50% decrease at 1.29 mM(coincubation)	Human skin	(Altikat et al., 2006)
Luteolin	50% decrease at 56 μM (coincubation)	Bovine liver catalase	(Krych and Gebicka, 2013)
Methylisothiazolinone	17.9%, 19.4% and 55.2% increase at 2, 4 and 8 μg/mL, respectively (24 h)	BEAS-2B cells	(Park and Seong, 2020)
Myricetin	50% decrease at 14 nM (coincubation)	Bovine liver catalase	(Krych and Gebicka, 2013)
Nidazole	50% decrease at 8.64 mM(coincubation)	Human skin	(Altikat et al., 2006)
Paraquat	28.5% decrease at 10 mM (10 min)	Rat Liver mitochondria	(Peixoto and Madeira, 2004)
Pioglitazone	Increase (max +200%) at 100, 200, 300, 400, 500 and 600 nM (3 min)	Bovine liver catalase	(Yekta et al., 2017)
Piroxicam	50% decrease at 414 μM (coincubation)	Human skin	(Altikat et al., 2006)
Pyrogallol	50% decrease at 74 μM (coincubation)	Bovine liver catalase	(Krych and Gebicka, 2013)
Quercetin	50% decrease at 33 μM (coincubation)	Bovine liver catalase	(Krych and Gebicka, 2013)
Retinoic acid	Increase at 100 nM and 1 μM (12 h and 24 h, respectively)	Rat Sertoli cells	(Pasquali et al., 2008)
Retinol	Increase at 5 μM (1 h), at 7 μM (12*h*) and at 5 and 7 μM (24 h)	Rat Sertoli cells	(Pasquali et al., 2008)
Rotenone	Decrease at 25–250 μM (24 h)	HepG2 cell line	(Siddiqui et al., 2013)
Rutin	50% decrease at 36 μM (coincubation)	Bovine liver catalase	(Krych and Gebicka, 2013)
Sodium Arsenite	Decrease at 10 and 20 μmol/L (24 h)	HaCaT cell line	(Sun et al., 2006)
Sodium azide	50% decrease at 1.22 μM (coincubation)	Bovine liver catalase	(Krych and Gebicka, 2013)
Sodium Sulfide	54.3% decrease at 100 μM (10 min)	*Salmonella typhimurium*	(Carlsson et al., 1988)
Sulfamethoxazole	50% decrease at 3.83 mM(concubation)	Human skin	(Altikat et al., 2006)
t-BHP	200% increase at 200, 500 μM (3 h)	HepG2 cell line	(Alía et al., 2005)
Titanium dioxide nanoparticles	31.4% and 46.3% decrease at 5 and 10 μg/mL (24 h), respectively	WISH cell line	(Saquib et al., 2012)

There are some critical points that can interfere with the quality of results, including the original quality of tissue homogenate or cell extraction, and the preservation of the samples on ice to avoid protein denaturation and loss of enzymatic activity. The total time necessary to perform the complete catalase activity assay, including extraction, homogenization and the kinetic assay, will significantly depend on the number of samples to process. The estimated time to process and determine catalase-activity in 10 tissue samples using our protocol is about 4 h. If liver samples are used, the total protocol can be split in 2 days since no decrease in catalase-activity was observed with the freezing process. If cell samples are used, they can be pelleted and frozen. Still, we recommend conducting the remaining protocol in the same day in which the cell pellet is resuspended in PB to prevent catalase activity loss.

CatBL solution and H_2O_2 solution must be freshly prepared to ensure the original properties. After H_2O_2 addition to the plate, it is crucial to immediately start the absorbance readings, so the results truly represent the maximal catalase activity. If the first kinetic point presents absorbance < 0.9, it means that H_2O_2 consumption has already occurred, and that maximal activity is not being measured. Performing an optimization step for sample amount is also recommended. A list of the main problems that may arise during the assay are outlined in Table S3.

The catalase activity will depend on tissue, specie, treatment and oxidative stress levels. Thus, it is difficult to predict a range of catalase activity. We have already optimized and used the catalase assay in several cell lines and in hepatic tissue from different sources (Table S2).

We observed in sheep liver extracts a decrease of absorbance around 0.6 throughout the time of the assay, corresponding to an activity of 1650 U/mg (27.5μkat/mg). Ibrahim et al. published results of catalase activity from several mice tissues (Ibrahim et al., 2000), presenting a lower activity in mice liver (883 ± 68 U/mg) when compared to our results. This difference in results is probably due to interspecies variation and from the more reliable data analysis method proposed in our work. Ibrahim et al. also described that kidney was the second tissue with higher catalase activity (377 ± 22 U/mg) followed by lung (116 ± 6 U/mg), heart (62.6 ± 6.8 U/mg), brain (8.9 ± 0.8 U/mg) and muscle (7.0 ± 1.5 U/mg) (Ibrahim et al., 2000).

The major limitation of the proposed protocol is that, without an automated device, it only allows the measurement of catalase activity in two samples each time which might increase the inter-assay variability. Moreover, the assay is not sensitive enough to measure samples with less than 11.5 U catalase what can compromise the application of this protocol to mice brain or muscle tissue samples (Ibrahim et al., 2000). In addition, the assay requires specific spectrophotometer and ultraviolet multi-well plates that cannot be reutilized.

Despite these limitations, our method can be efficiently used in small amounts of specific samples in a robust, sensitive, time-saving and cost-effective manner to determine the catalase kinetic-activity in biomedicine and toxicology approaches.

Funding

Funded by ERDF funds through the Operational Programme Competitiveness Factors – COMPETE2020 and national funds by Foundation for Science and Technology under FCT-Post-doctoral Fellowship (SPP, SFRH/BPD/116061/2016), project grant PTDC/DTP-DES/1082/2014(POCI-01-0145-FEDER-016657), PTDC/BTM-SAL/29297/2017-POCI-01-0145-FEDER-029297, PTDC/MED-FAR/29391/2017-POCI-01-0145-FEDER-029391, PTDC/BIA-MOL/28607/2017, POCI-01-0145-FEDER-028607, LFG was supported by project “Summer Course in Interdisciplinary Research, Development and Innovation in Cellular and Molecular Metabolism” (15-20/7/245), funded by the Portuguese Foundation for Science and Technology (FCT) and Directorate General for Higher Education (DGES), strategic project UIDB/04539/2020, and NIH grant R01HD070096-01A1. The funding agencies had no role in study design, data collection and analysis, decision to publish, or preparation of this document.

Declaration of Competing Interest

No conflict of interests to declare.

Acknowledgements

The author acknowledges the comments from Cláudia Deus, José Teixeira, Ricardo Amorim, and Ricardo Marques.

Appendix A. Supplementary data

Supplementary data to this article can be found online at https://doi.org/10.1016/j.tiv.2020.104996.

References

Aebi, H., 1984. [13] Catalase in vitro. Methods Enzymol. **105**, 121–126.
Alía, M., Ramos, S., Mateos, R., Bravo, L., Goya, L., 2005. Response of the antioxidant defense system to tert-butyl hydroperoxide and hydrogen peroxide in a human hepatoma cell line (HepG2). J. Biochem. Mol. Toxicol. 19, 119–128.
Al-Suhaimi, E., 2014. Molecular mechanisms of leptin and pro-apoptotic signals induced by menadione in HepG2 cells. Saudi J. Biol. Sci. 21, 582–588.
Altikat, S., Coban, A., Ciftci, M., Ozdemir, H., 2006. In vitro effects of some drugs on catalase purified from human skin. J. Enzyme Inhib. Med. Chem. 21, 231–234.
Arif, A., Salam, S., Mahmood, R., 2020. Bioallethrin-induced generation of reactive species and oxidative damage in isolated human erythrocytes. Toxicol. in Vitro 65, 104810.
Bhatti, J.S., Bhatti, G.K., Reddy, P.H., 2017. Mitochondrial dysfunction and oxidative stress in metabolic disorders — a step towards mitochondria based therapeutic strategies. Biochim. Biophys. Acta Mol. basis Dis. 1863, 1066–1077.
Bukowska, B., Michałowicz, J., Duda, W., 2007. Alterations in human red blood cell properties induced by 3-(dimethylamino)phenol (in vitro). Toxicol. in Vitro 21, 1574–1580.
Cao, C., Leng, Y., Kufe, D., 2003a. Catalase activity is regulated by c-Abl and Arg in the oxidative stress response. J. Biol. Chem. 278, 29667–29675.
Cao, C., et al., 2003b. Catalase is regulated by ubiquitination and proteosomal degradation. Role of the c-Abl and Arg tyrosine kinases. Biochemistry 42, 10348–10353.
Carlsson, J., Berglin, E.H., Claesson, R., Edlund, M.B.K., Persson, S., 1988. Catalase inhibitiob by sulfide and hydrogen peroxide-induced mutagenicity in Salmonella typhimurium strain TA102. Mutat. Res. Fundam. Mol. Mech. Mutagen. 202, 59–64.
Coalova, I., Ríos Molina de del, M.C., Chaufan, G., 2014. Influence of the spray adjuvant on the toxicity effects of a glyphosate formulation. Toxicol. in Vitro 28, 1306–1311.
Dawson, J., 1990. Handbook of enzyme inhibitors. Biochem. Educ. 18, 156.
De Luca, C., Valls, G.B., Mason, J.A., 1970. Drug effects on catalase activity in the mammalian cell. The role of the cell in drug action. Biochem. Pharmacol. 19, 2211–2220.
Dunning, S., et al., 2013. Glutathione and antioxidant enzymes serve complementary roles in protecting activated hepatic stellate cells against hydrogen peroxide-induced cell death. Biochim. Biophys. Acta Mol. basis Dis. 1832, 2027–2034.
Furuta, H., Hachimori, A., Ohta, Y., Samejima, T., 1974. Dissociation of bovine liver catalase into subunits on acetylation. J. Biochem. 76, 481–491.
Gargouri, B., et al., 2020. Bifenthrin insecticide promotes oxidative stress and increases inflammatory mediators in human neuroblastoma cells through NF-kappaB pathway. Toxicol. in Vitro 65, 104792.
Ghavamipour, F., Sajedi, R.H., Khajeh, K., 2018. A chemiluminescence-based catalase assay using H2O2-sensitive CdTe quantum dots. Microchim. Acta 185, 376.
Ghosh, P., Roy, S.S., Chakraborty, P., Ghosh, S., Bhattacharya, S., 2013. Effects of organoselenium compound 2-(5-selenocyanatopentyl)- benzo[de]isoquinoline 1,3-dione on cisplatin induced nephrotoxicity and genotoxicity: an investigation of the influence of the compound on oxidative stress and antioxidant enzyme system. BioMetals 26, 61–73.
Glorieux, C., Calderon, P.B., 2017. Catalase, a remarkable enzyme: targeting the oldest antioxidant enzyme to find a new cancer treatment approach. Biol. Chem. 398, 1095–1108.
Glorieux, C., Zamocky, M., Sandoval, J.M., Verrax, J., Calderon, P.B., 2015. Regulation of catalase expression in healthy and cancerous cells. Free Radic. Biol. Med. 87, 84–97.
Gonçalves, A.C., et al., 2013. Oxidative stress mediates apoptotic effects of ascorbate and dehydroascorbate in human Myelodysplasia cells in vitro. Toxicol. in Vitro 27, 1542–1549.
Halliwell, B., Gutteridge, J.M.C., 2015. Free Radicals in Biology and Medicine. Oxford University Presshttps://doi.org/10.1093/acprof:oso/9780198717478.001.0001.
Herpers, B., et al., 2016. Activation of the Nrf2 response by intrinsic hepatotoxic drugs correlates with suppression of NF-κB activation and sensitizes toward TNFα-induced cytotoxicity. Arch. Toxicol. 90, 1163–1179.
Ibrahim, W., Lee, U.S., Yen, H.C., St Clair, D.K., Chow, C.K., 2000. Antioxidant and oxidative status in tissues of manganese superoxide dismutase transgenic mice. Free Radic. Biol. Med. 28, 397–402.
Jakopitsch, C., et al., 2003. The catalytic role of the distal site asparagine-histidine couple in catalase-peroxidases. Eur. J. Biochem. 270, 1006–1013.
Krych, J., Gebicka, L., 2013. Catalase is inhibited by flavonoids. Int. J. Biol. Macromol. 58, 148–153.
Kubota, Y., Takahashi, S., Sato, H., 2004. Significant contamination of superoxide dismutases and catalases with lipopolysaccharide-like substances. Toxicol. in Vitro 18, 711–718.
Lennicke, C., Rahn, J., Lichtenfels, R., Wessjohann, L.A., Seliger, B., 2015. Hydrogen peroxide - production, fate and role in redox signaling of tumor cells. Cell Commun. Signal. 13, 1–19.
Li, Y., et al., 2017. Novel lipidic and bienzymatic nanosomes for efficient delivery and enhanced bioactivity of catalase. Int. J. Pharm. 532, 157–165.
Lim, S., et al., 2018. Meroterpenoid-rich fraction of the ethanolic extract from sargassum serratifolium suppressed oxidative stress induced by tert-butyl hydroperoxide in HepG2 cells. Mar. Drugs 16.
Maćczak, A., Cyrkler, M., Bukowska, B., Michałowicz, J., 2017. Bisphenol a, bisphenol S, bisphenol F and bisphenol AF induce different oxidative stress and damage in human red blood cells (in vitro study). Toxicol. in Vitro 41, 143–149.
Macêdo, D.S., et al., 2005. Cocaine alters catalase activity in prefrontal cortex and striatum of mice. Neurosci. Lett. 387, 53–56.
Machado, Nuno G., Baldeiras, Inês, Pereira, Gonçalo C., Pereira, Susana P., Oliveira, Paulo J., 2010. Sub-chronic administration of doxorubicin to Wistar rats results in oxidative stress and unaltered apoptotic signaling in the lung. Chemico-Biological Interactions journal 188, 478–486. https://doi.org/10.1016/j.cbi.2010.09.027. http://www.ncbi.nlm.nih.gov/pubmed/20932959 20932959, In press.
Marinho, H.S., Real, C., Cyrne, L., Soares, H., Antunes, F., 2014. Hydrogen peroxide sensing, signaling and regulation of transcription factors. Redox Biol. 2, 535–562.
Moloney, J.N., Cotter, T.G., 2018. ROS signalling in the biology of cancer. Semin. Cell Dev. Biol. 80, 50–64.
Mu, J., Wang, Y., Zhao, M., Zhang, L., 2012. Intrinsic peroxidase-like activity and catalase-like activity of Co3O4 nanoparticles. Chem. Commun. 48, 2540–2542.
Nenoi, M., Ichimura, S., Yukawa, O., Mita, K., Cartwright, I.L., 2001. Regulation of the catalase gene promoter by Sp1, CCAAT-recognizing factors, and a WT1/Egr-related factor in hydrogen peroxide-resistant HP100 cells. Cancer Res. 61, 5885–5894.

Paradies, G., Paradies, V., Ruggiero, F.M., Petrosillo, G., 2014. Oxidative stress, cardiolipin and mitochondrial dysfunction in nonalcoholic fatty liver disease. World J. Gastroenterol. 20, 14205–14218.
Park, E.J., Seong, E., 2020. Methylisothiazolinone induces apoptotic cell death via matrix metalloproteinase activation in human bronchial epithelial cells. Toxicol. in Vitro 62, 104661.
Pasquali, M.A.B., et al., 2008. Retinol and retinoic acid modulate catalase activity in Sertoli cells by distinct and gene expression-independent mechanisms. Toxicol. in Vitro 22, 1177–1183.
Peixoto, F., Madeira, M.C., 2004. A Comparative Study of Plant and Animal Mitochondria Exposed to Paraquat Reveals that Hydrogen Peroxide is not Related to the Observed Toxicity. 18. pp. 733–739.
Radi, R., et al., 1991. Detection of catalase in rat heart mitochondria. J. Biol. Chem. 266, 22028–22034.
Rafikov, R., et al., 2014. Endothelin-1 stimulates catalase activity through the PKCδ-mediated phosphorylation of serine 167. Free Radic. Biol. Med. 67, 255–264.
Rindler, P.M., Plafker, S.M., Szweda, L.I., Kinter, M.G., 2013. High dietary fat selectively increases catalase expression within cardiac mitochondria. J. Biol. Chem. 288, 1979–1990.
Salvi, M., et al., 2007. Catalase takes part in rat liver mitochondria oxidative stress defense. J. Biol. Chem. 282, 24407–24415.
Saquib, Q., et al., 2012. Titanium dioxide nanoparticles induced cytotoxicity, oxidative stress and DNA damage in human amnion epithelial (WISH) cells. Toxicol. in Vitro 26, 351–361.
Schieber, M., Chandel, N.S., 2014. ROS function in redox signaling and oxidative stress. Curr. Biol. 24, R453–R462.
Sepasi Tehrani, H., Moosavi-Movahedi, A.A., 2018. Catalase and its mysteries. Prog. Biophys. Mol. Biol. 140, 5–12.
Shabalala, S.C., et al., 2019. Aspalathin ameliorates doxorubicin-induced oxidative stress in H9c2 cardiomyoblasts. Toxicol. in Vitro 55, 134–139.
Siddiqui, M.A., et al., 2013. Rotenone-induced oxidative stress and apoptosis in human liver HepG2 cells. Mol. Cell. Biochem. 384, 59–69.
Sies, H., 2017. Hydrogen peroxide as a central redox signaling molecule in physiological oxidative stress: oxidative eustress. Redox Biol. 11, 613–619.
Sun, X., et al., 2006. Effects of sodium arsenite on catalase activity, gene and protein expression in HaCaT cells. Toxicol. in Vitro 20, 1139–1144.
Switala, J., Loewen, P.C., 2002. Diversity of properties among catalases. Arch. Biochem. Biophys. 401, 145–154.
Takeda, A., Miyahara, T., Hachimori, A., Samejima, T., 1980. The interactions of thiol compounds with porcine erythrocyte catalase. J. Biochem. 87.
Teixeira, J.A., Mota, M., 1992. Determination of catalase activity and its inhibition by a simple manometric method. Biochem. Educ. 20, 174–175.
Terada, M. [Sodium azide], 2004. Nihon Rinsho 62 (Suppl. 1), 539–544.
Veal, E.A., Day, A.M., Morgan, B.A., 2007. Hydrogen peroxide sensing and signaling. Mol. Cell Rev. https://doi.org/10.1016/j.molcel.2007.03.016.
Weydert, C.J., Cullen, J.J., 2010. Measurement of superoxide dismutase, catalase and glutathione peroxidase in cultured cells and tissue. Nat. Protoc. 5, 51–66.
Xiao, W., Goswami, P.C., 2015. Down-regulation of peroxisome proliferator activated receptor γ coactivator 1α induces oxidative stress and toxicity of 1-(4-Chlorophenyl)-benzo-2,5-quinone in HaCaT human keratinocytes. Toxicol. in Vitro 29, 1332–1338.
Yan, H., Harding, J.J., 1997. Glycation-induced inactivation and loss of antigenicity of catalase and superoxide dismutase. Biochem. J. 328 (Pt 2), 599–605.
Yang, B., Hao, F., Li, J., Chen, D., Liu, R., 2013. Binding of chrysoidine to catalase: spectroscopy, isothermal titration calorimetry and molecular docking studies. J. Photochem. Photobiol. B Biol. 128, 35–42.
Yekta, R., Dehghan, G., Rashtbari, S., Sheibani, N., Moosavi-Movahedi, A.A., 2017. Activation of catalase by pioglitazone: multiple spectroscopic methods combined with molecular docking studies. J. Mol. Recognit. 30, e2648.
Zhao, M.X., Wen, J.L., Wang, L., Wang, X.P., Chen, T.S., 2019. Intracellular catalase activity instead of glutathione level dominates the resistance of cells to reactive oxygen species. Cell Stress Chaperones 24, 609–619.
Zhen, W., et al., 2018. BSA-IrO2: catalase-like nanoparticles with high photothermal conversion efficiency and a high X-ray absorption coefficient for anti-inflammation and antitumor theranostics. Angew. Chem. Int. Ed. 57, 10309–10313.